Received: 12 June 2020 | Revised: 16 October 2020 | Accepted: 17 November 2020

DOI: 10.1111/bph.15333

RESEARCH PAPER - THEMED ISSUE

Stimulation of soluble guanylyl cyclase (sGC) by riociguat attenuates heart failure and pathological cardiac remodelling

Julia Rüdebusch[1,2] | Alexander Benkner[1,2] | Neetika Nath[3] | Lina Fleuch[1,2] | Lars Kaderali[2,3] | Karina Grube[1,2] | Karin Klingel[4] | Gertrud Eckstein[5] | Thomas Meitinger[5] | Jens Fielitz[1,2] | Stephan B. Felix[1,2]

[1]Department of Internal Medicine B, University Medicine Greifswald, Greifswald, Germany

[2]DZHK (German Centre for Cardiovascular Research, partner site Greifswald), Greifswald, Germany

[3]Institute of Bioinformatics, University Medicine Greifswald, Greifswald, Germany

[4]Cardiopathology, Institute for Pathology, University Hospital Tübingen, Tübingen, Germany

[5]Institute of Human Genetics, Helmholtz Zentrum München, Neuherberg, Germany

Correspondence
Stephan B. Felix, Department of Cardiology and Internal Medicine B, University Medicine Greifswald, Ferdinand-Sauerbruchstrasse, 17475 Greifswald, Germany.
Email: stephan.felix@med.uni-greifswald.de

Funding information
Deutsches Zentrum für Herz-Kreislaufforschung, Grant/Award Number: DZHK 81Z5400153

Background and Purpose: Heart failure is associated with an impaired NO–soluble guanylyl cyclase (sGC)–cGMP pathway and its augmentation is thought to be beneficial for its therapy. We hypothesized that stimulation of sGC by the sGC stimulator riociguat prevents pathological cardiac remodelling and heart failure in response to chronic pressure overload.

Experimental Approach: Transverse aortic constriction or sham surgery was performed in C57BL/6N mice. After 3 weeks of transverse aortic constriction when heart failure was established, animals receive either riociguat or its vehicle for 5 additional weeks. Cardiac function was evaluated weekly by echocardiography. Eight weeks after surgery, histological analyses were performed to evaluate remodelling and the transcriptome of the left ventricles (LVs) was analysed by RNA sequencing. Cell culture experiments were used for mechanistically studies.

Key Results: Transverse aortic constriction resulted in a continuous decrease of LV ejection fraction and an increase in LV mass until week 3. Five weeks of riociguat treatment resulted in an improved LV ejection fraction and a decrease in the ratio of left ventricular mass to total body weight (LVM/BW), myocardial fibrosis and myocyte cross-sectional area. RNA sequencing revealed that riociguat reduced the expression of myocardial stress and remodelling genes (e.g. *Nppa*, *Nppb*, *Myh7* and collagen) and attenuated the activation of biological pathways associated with cardiac hypertrophy and heart failure. Riociguat reversed pathological stress response in cultivated myocytes and fibroblasts.

Conclusion and Implications: Stimulation of the sGC reverses transverse aortic constriction-induced heart failure and remodelling, which is associated with improved myocardial gene expression.

KEYWORDS

cGMP signalling, heart failure, riociguat, RNA sequencing, soluble GC, TAC

Abbreviations: DEGs, differentially expressed genes; HF, heart failure; LV, left ventricle; NCM, neonatal rat cardiomyocyte; Rio, riociguat; sGC, soluble guanylyl cyclase; Sol, solvent; TAC, transverse aortic constriction.

1 | INTRODUCTION

Heart failure (HF) is a pervasive cause of morbidity and mortality worldwide and is the leading cause of hospitalization in Europe and the United States (Ambrosy et al., 2014). The prevalence of heart failure is increasing due to the aging population and the prolongation of life expectancy (Ponikowski et al., 2016). In the last decades, heart failure treatments have improved survival and have reduced hospitalization rates, but outcome remains poor pointing towards the need of novel treatments. The progression of heart failure is accompanied by numerous structural and molecular changes in the myocardium such as myocyte hypertrophy, interstitial and perivascular fibrosis, reorganization of the cytoskeleton and activation of the fetal gene program (Barry, Davidson, & Townsend, 2008). A better understanding of the molecular pathways involved in heart failure is crucial to establish novel heart failure medications. Previously, the **NO–soluble GC** (sGC)–**cGMP** pathway was shown to be impaired in heart failure and its restoration was suggested as an attractive pharmacological target in heart failure (Gheorghiade et al., 2013; Sandner, 2018). Specifically, NO is an important regulator of vascular tone, capillary permeability and platelet adhesion. It is generated by **endothelial NOS** (eNOS), which is activated by hormonal and physical stimuli (Sandner, 2018). Once released, NO diffuses into smooth muscle cells and stimulates the sGC that catalyses the conversion of guanosine triphosphate (GTP) into cGMP. cGMP acts as a second messenger to regulate numerous physiological actions, such as smooth muscle relaxation via activation of **PKG** signalling. Heart failure is associated with endothelial dysfunction and reduced bioavailability of NO with insufficient stimulation of sGC and reduced production of cGMP (Gheorghiade et al., 2013; Ghofrani et al., 2017). The impairment of the NO–sGC–cGMP pathway consequently results in vasoconstriction, platelet aggregation, inflammation, fibrosis and, most importantly, maladaptive cardiac hypertrophy (Ghofrani et al., 2017). Accordingly, restoration of the NO–sGC–cGMP pathway is an attractive pharmacological target for heart failure therapy. **Riociguat** is an NO-independent stimulator of the sGC that sensitizes the sGC to endogenous NO and directly stimulates sGC to produce cGMP. We hypothesized that riociguat reverses pathological effects that accompany chronic pressure overload-induced cardiac hypertrophy, which eventually leads to heart failure.

We tested the effects of the sGC stimulator riociguat on myocardial contractile function, hypertrophy and remodelling in an *in vivo* mouse model of chronic pressure overload caused by transverse aortic constriction (TAC). To determine whether riociguat reverses the molecular changes caused by TAC, the left ventricular (LV) gene expression profile of TAC-operated mice treated with and without riociguat was analysed by RNA sequencing. Our data revealed that sGC stimulation reverses the effect of TAC on cardiac hypertrophy, fibrosis and LV function as well as on myocardial gene expression.

What is already known

- Heart failure (HF) is associated with reduced bioavailability of NO and insufficient stimulation of sGC.
- sGC stimulators are anti-inflammatory and anti-fibrotic and may serve as novel heart failure therapies.

What this study adds

- Our experimental study shows that the sGC stimulator riociguat improves myocardial function.
- sGC stimulation reverses remodelling in a mouse model of pressure overload-induced HF.

What is the clinical significance

- sGC stimulation with vericiguat reduces cardiovascular death and HF hospitalization in HFrEF patients (VICTORIA trial).
- Our data show that the sGC stimulator riociguat improves pressure overload-induced HF in mice.

2 | METHODS

2.1 | Animals

All experiments were performed with 8-week-old male C57BL/6N wild-type mice (Charles River Laboratories, Sulzfeld, Germany; RRID: MGI:5651595). The mice were kept in a temperature-controlled animal facility with a 12-h light/dark cycle and free access to food and water. No more than five mice were housed in one cage. All procedures were approved by the local animal committee (permit number: LALLF 7221.3-1-00/16). Animal experiments were performed in conformity with the Directive 2010/63/EU of the European Parliament and of the Council of 22 September 2010 on the protection of animals used for scientific purposes. Animal studies are reported in compliance with the ARRIVE guidelines (Percie du Sert et al., 2020) and with the recommendations made by the *British Journal of Pharmacology* (Lilley et al., 2020).

2.1.1 | Animal study design

Eight-week-old male C57BL/6N mice underwent either transverse aortic constriction (TAC) or sham surgery. For surgery, mice were initially anaesthetized with 3% **isoflurane**, intubated, ventilated (2% isoflurane in air, 50 ml·min^{-1}; rodent MiniVent, Harvard Apparatus,

Germany) and maintained under normothermic conditions with the use of a heating pad. The thoracic cavity was opened by a median sternotomy until the third rib and a blunted needle (26 G) was placed on the aortic arch between the innominate artery and left common carotid. A 7–0 suture was tied around the needle and the aortic arch. Immediately afterwards, the needle was removed and the thoracic cavity was closed. Similarly, the sham surgery was performed except knotting the suture. Before and over a period of 3 days (every 12 h) after surgery, the animals were treated with analgesic medication (buprenorphine 0.02 mg·kg^{-1} s.c.) and monitored daily until the end of the study. All mice were subjected to transthoracic echocardiography (Vevo® 2100, FUJIFILM VisualSonics®, Inc.) to measure cardiac function before and weekly after surgery until the end of the study (Figure 1a). Animals were sedated using 3% isoflurane and maintained under normothermic conditions with the use of a heating pad and low isoflurane (~1.5%). M-mode tracings of the left ventricle (LV) were acquired using the parasternal short-axis view, with the ultrasound beam perpendicular to the LV at the midpapillary level. M-mode tracing (Vevo® LAB 3.0.0 software, Visual Sonics®) was used to determine LV ejection fraction (LVEF), LV fractional shortening (LVFS), LV end-diastolic volume (LVEDV), LV end-systolic volume (LVESV), LV inner diameter in systole (LVIDs) and diastole (LVIDd), and LV mass (LVM). Pulse wave Doppler was used to measure the peak aortic velocity at the level of the banding. The aortic peak pressure gradient was calculated by using the peak aortic velocity according to the following formula (Harris & Kuppurao, 2016), $4x\left(\frac{\text{Peak aortic velocity}}{1{,}000}\right)^2$. Only TAC mice were included that exhibited a

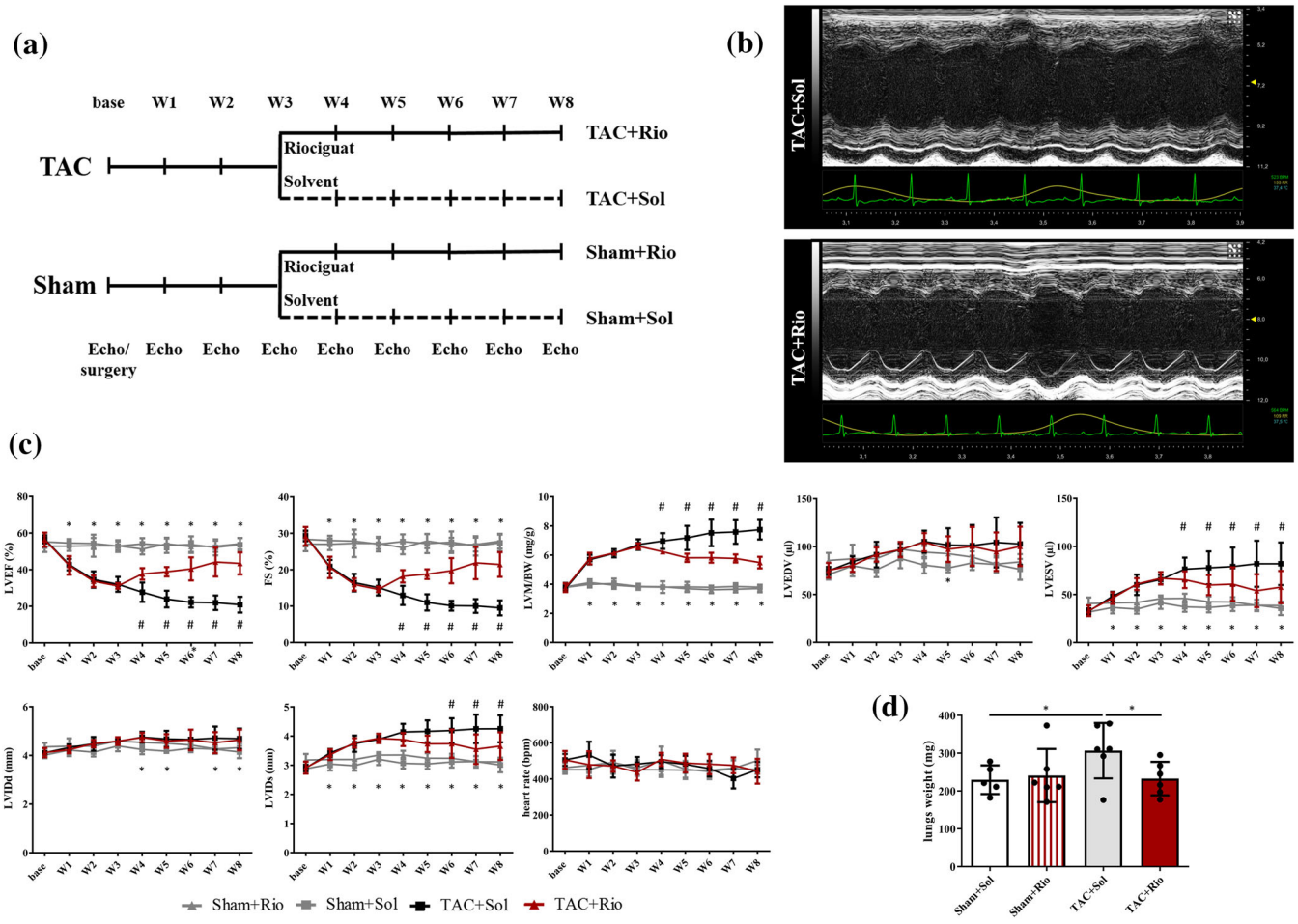

FIGURE 1 Riociguat reverses transverse aortic constriction (TAC)-induced heart failure. (a) Experimental design overview. (b) Representative M-mode echocardiograms of short-axis views of hearts after 8 weeks of TAC treated with solvent (TAC + Sol, upper panel) and riociguat (TAC + Rio, lower panel). (c) Echocardiographic analysis of solvent- and riociguat-treated TAC-operated mice and of solvent- and riociguat-treated sham-operated mice. TAC surgery caused a reduction in left ventricular (LV) ejection fraction (LVEF) and LV fractional shortening (LVFS) and an increase in LV mass to body weight ratio (LVM/BW), LV end-systolic volume (LVESV) and LV end-systolic internal dimension (LVIDs) compared to sham-treated animals. Without affecting the heart rate, riociguat treatment attenuated these effects in TAC mice compared to solvent-treated TAC animals. LV end-diastolic volume (LVEDV) and LV end-diastolic internal dimension (LVIDd) were not affected by riociguat. $n = 6$ per group. All data are expressed as mean ± SD (TAC + Sol vs. Sham + Sol: $^{*}P < 0.05$; TAC + Rio vs. TAC + Sol: $^{\#}P < 0.05$). (d) TAC led to an increased lung weight after 8 weeks, which was significantly reduced when mice were treated with riociguat ($^{*}P < 0.05$). $n = 6$ per group. All data are expressed as mean ± SD

peak velocity ≥4,000 mm·s^{-1}, in accordance with a pressure gradient of ≥64 mmHg. The mean pressure gradient of all TAC mice, which were included, was comparable between the groups (TAC + Rio [mean ± SD]: 77.1 ± 3.5 mmHg vs. TAC + Sol 76.8 ± 5.5 mmHg, P = 0.91; Figure S1).

To test the therapeutic potential of riociguat, we first induced heart failure, cardiac hypertrophy and remodelling by 3 weeks of chronic pressure overload. At day 21, mice were randomized to riociguat or solvent/vehicle (Sol; Transcutol®/Cremaphor®/water: 10%/20%/70%) treatment, resulting in four treatment groups (n = 6 per group):- sham solvent (Sham + Sol), sham riociguat (Sham + Rio), TAC solvent (TAC + Sol) and TAC riociguat (TAC + Rio). The dosage of riociguat was set to 3 mg·kg^{-1}, as used previously in other studies (Dees et al., 2015; Geschka et al., 2011; Ott et al., 2012; Pichl et al., 2019; Sharkovska et al., 2010). Riociguat (Adempas® purchased from Bayer Healthcare, Germany) or Sol was administered daily by oral gavage until the end of the study at day 56 (Figure 1a). After 8 weeks (day 56), the mice were killed, blood samples were taken and the hearts were perfused with ice-cold PBS. The free wall of the LV was snap-frozen and stored at −80°C until analysis and whole hearts were fixed in 4% paraformaldehyde and paraffin embedded.

Echocardiographic acquisition (K.G.) and echocardiographic data analysis (J.R.) were examined by an observer blinded to treatment.

2.1.2 | Mortality and randomization

Twenty-six mice underwent TAC surgery. Four mice died during surgery resulting in 22 TAC mice included in the study. Until day 21, four mice died, resulting in 18 mice that were 1:1 randomized to receive either Rio or Sol. One mouse of the Rio group died after 5 weeks. At the end, there were eight TAC mice in the Rio group and nine TAC mice in the Sol group. One mouse in the Rio group and two mice in the Sol group did not reach sufficient stenosis as indicated by a pressure gradient below our cut-off of 64 mmHg. From seven mice in each TAC group, six were randomly assigned for analysis. In the sham group, 18 mice were operated and no mouse died. From nine mice in each sham group, six from each group were randomly assigned for analysis.

2.2 | Histological analysis

Three paraffin sections per heart (5 μm, six hearts per group) were stained with picrosirius red stain kit (Scy Tek Laboratories, Logan, Utah, USA) according to the manufacturer's protocol to visualize collagen fibres. Each heart section was captured entirely using single field images, which were merged into a single macro image (BZ 9000 Microscope, Keyence, Germany). Percentage area of fibrosis was analysed by an observer (K.G), blinded to treatment, using colour determination software (BZ II Analyzer, Keyence, Germany).

To determine myocyte cross-sectional area, two cryosections per heart (6 μm, six hearts per group) were prepared and fluorescence staining using anti-dystrophin monoclonal antibody (clone D8043, Sigma Aldrich; RRID:AB_259241) and secondary anti-mouse antibody (Alexa 488, Invitrogen) was performed. Two images of each section were analysed by an observer (K.G.) blinded to treatment, tracing 80 cross-sectioned myocytes per heart (NIH ImageJ software, RRID:SCR_003070, Rueden et al., 2017).

2.3 | RNA isolation and RNA sequencing

RNA was isolated from the free wall of the LV, using miRNeasy Mini Kit (Qiagen) according to the manufacturer's protocol. Quality and concentration of RNA were determined using Agilent Bioanalyzer 2100 with Agilent RNA 6000 Nano Kit according to the Eukaryote Total RNA Nano Series II protocol.

For mRNA library preparation, 1 μg of total RNA per sample (n = 6 per group) was used. Library construction was performed as described in the high-throughput protocol of the TruSeq stranded mRNA Sample Prep Guide (Illumina®) in an automated manner using the Bravo Automated Liquid Handling Platform (Agilent). CDNA libraries were assessed for quality and quantity with the Lab Chip GX (Perkin Elmer) and the Quant-iT PicoGreen dsDNA Assay Kit (Life Technologies). RNA libraries were multiplexed and sequenced on seven lanes as 100-bp paired-end run on an Illumina HiSeq4000 platform. On average, we produced about 8 Gb of sequence per sample.

For bioinformatics data analysis, Trimmomatric (V 0.35) package and FASTQC were used for data quality assessment. During the trimming step, leading and trailing reads and PHRED score lower than 3 were removed by choosing parameters called LEADING:3 and TRAILING:3 in the Trimmomatric package. TopHat was used for alignment against the mouse reference genome (10 mm). Differential expression was computed with the DESeq2 package (RRID:SCR_015687) and for annotation, we used the AnnotationDbi package, which are available in Bioconductor R (RRID:SCR_006442) program. The Wald statistic (Chen et al., 2011) was used to perform statistical analysis to observe whether the difference between two conditions is significant. Benjamini–Hochberg correction was used to compute adjusted P values. An adjusted P value (q value) of 0.05 implies that we are willing to accept that 5% of the tests found to be statistically significant will be false positives. All RNA-Seq fastq data are available at the Sequence Read Archive (BioSample accession SAMN13337567). Further, we incorporated filtering steps in which genes with no expression and less than three reads were removed. Also, we removed genes with at least four biological replicates that show expression with more than three reads.

For validation of the RNA sequencing data and expression analysis of neonatal myocytes, the expression of a subset of genes was analysed using NanoString nCounter™ Analysis System (NanoString Technologies®, Seattle, USA; RRID:SCR_003407) according to the manufacturer's protocol (Supporting Information Material and Methods and Figure S2). mRNA expression was normalized to a geometric mean of five housekeeping genes (*Rpl4*, *Polr2a*, *Rpl32*, *Hprt1* and *Gapdh*).

2.4 | Cell culture

Compositions of solutions and media are listed in the supporting information. The neonatal cardiomyocytes (NCMs) and fibroblasts were isolated from 1- to 3-day-old Wistar rats. Whole hearts were dissociated and digested with collagenase–pancreatin suspension. The cells were resuspended in neonatal cardiomyocytes culture medium (NCM-CM), pre-plated on petri dishes and incubated for 1 h to separate the fibroblasts from the NCM. NCMs were then cultured in NCM-CM on pre-coated (0.1% gelatin) dishes. Fibroblasts were cultured in supplemented DMEM.

2.4.1 | Analysis of cardiomyocyte hypertrophy in vitro

After 48 h of isolation, NCMs were treated in Panserin starvation medium (PAN, Biotech), with either 10 nM of **angiotensin II** (Ang II), 100 nM of riociguat (Sigma-Aldrich) or the combination of both for further 48 h (Dees et al., 2015; Reinke et al., 2015; Reiss et al., 2015). After fixing with 2% paraformaldehyde, cells were stained with anti-α-actinin (clone EA-53, 1:1,000; Sigma-Aldrich; RRID:AB_2221571) and exposed to secondary antibody conjugated to Alexa Fluor 488 (1:200; Invitrogen, Karlsruhe, Germany; RRID:AB_2534069). Nuclei were stained with **DAPI** (RRID:AB_2307445; 0.2 $\mu g \cdot ml^{-1}$, Roth, Karlsruhe, Germany). Blinded to the observer (L.F.), five random pictures per well (three wells per condition) were taken with the Keyence BZ-9000 fluorescence microscope and analysed by BZ II Analyzer Software. The total area was divided by the number of cells to receive the mean size of the cells.

2.4.2 | Fibroblast proliferation assay

Fibroblasts were cultured in DMEM supplemented in 96-well plates (2,500 cells per well) for 24 h and treated with 10-nM Ang II, 100-nM riociguat (Sigma-Aldrich) or the combination of both for further 48 h. Fibroblast proliferation was analysed by a CCK8 assay (Cell Counting Kit-8, Sigma-Aldrich) according to the manufacturer's protocol.

2.5 | Data and statistical analysis

The data and statistical analysis comply with the recommendations of the *British Journal of Pharmacology* on experimental design and analysis in pharmacology (Curtis et al., 2018). In all analysis, the number of independent experiments was at least 6 (exact numbers are provided in the figure legends), except in Figure 2b showing data from experimental day 21, providing unpublished data of an earlier study (Rüdebusch et al., 2017) and without exclusions for outlying data points employed.

Transcripts were identified as differentially expressed in two comparisons: (i) transcripts that are up-regulated or down-regulated by 20%, for a false discovery rate (FDR) of 5% or less ($q < 0.05$); (ii) for Ingenuity® Pathway *Z*-Score Analysis (IPA®, QIAGEN Redwood City, www.qiagen.com/ingenuity; RRID:SCR_008653), transcripts with an up-regulation or down-regulation of at least 20% and FDR of 25% or less were included. Canonical pathway expression analysis comprised all differentially expressed genes (DEGs) with an FDR of less than 5% ($q < 0.05$). All data are expressed as mean ± SD. For group comparisons of echocardiographic parameters, fibrosis, myocyte cross-sectional area and in vitro hypertrophy and proliferation, we employed a one-way ANOVA with Newman–Keuls post hoc test. The post hoc tests were conducted only if F in ANOVA achieved $P < .05$ and there was no significant variance inhomogeneity. For gene expression analysis in NCM, a Student's *t*-test was used. The level of significance is provided in the figure legend. All analyses used GraphPad Prism (8.1.1; GraphPad Software, RRID:SCR_002798, Inc., San Diego, CA). Where the data are presented as bar charts, an examination of the individual data did not reveal any unusual or interesting aspects of the data that are not made obvious from the bar chart (George et al., 2017).

2.6 | Nomenclature of targets and ligands

Key Key protein targets and ligands in this article are hyperlinked to corresponding entries in the IUPHAR/BPS Guide to PHARMACOLOGY http://www.guidetopharmacology.org and are permanently archived in the Concise Guide to PHARMACOLOGY 20119/20 (Alexander et al., 2019).

3 | RESULTS

3.1 | Riociguat improves cardiac function and attenuates pathological cardiac remodelling and hypertrophy

Three weeks of TAC resulted in a continuous decrease of LVEF (from 56.6 ± 2.2% to 32.0 ± 4.1%) and LVFS (from 29.3 ± 1.5% to 15.1 ± 2.2%). Riociguat treatment (TAC + Rio group) led to a significant recovery of LVEF and LVFS, whereas the solvent-treated TAC mice (TAC + Sol group) showed a further decline in both parameters until week 8 (Figure 1c). The heart rate did not differ between all experimental groups during follow-up. Concomitantly, LVESV (82.0 ± 22.0 µl vs. 57.7 ± 16.9 µl) and LVIDs (4.2 ± 0.5 mm vs. 3.7 ± 0.5 mm) were significantly reduced in riociguat-treated TAC animals. LVEDV and LVIDs showed a trend towards a decrease, which did not reach statistical significance. The increase in the LVM to body weight ratio (LVM/BW) after TAC was significantly attenuated by riociguat treatment (Figure 1c). Furthermore, after 8 weeks of TAC, the lung weight of TAC + Rio mice was significantly lower when compared to the TAC + Sol group (Figure 1d).

LV pressure overload is associated with increased interstitial fibrosis and accumulation of collagen (Fielitz et al., 2001, 2008). As

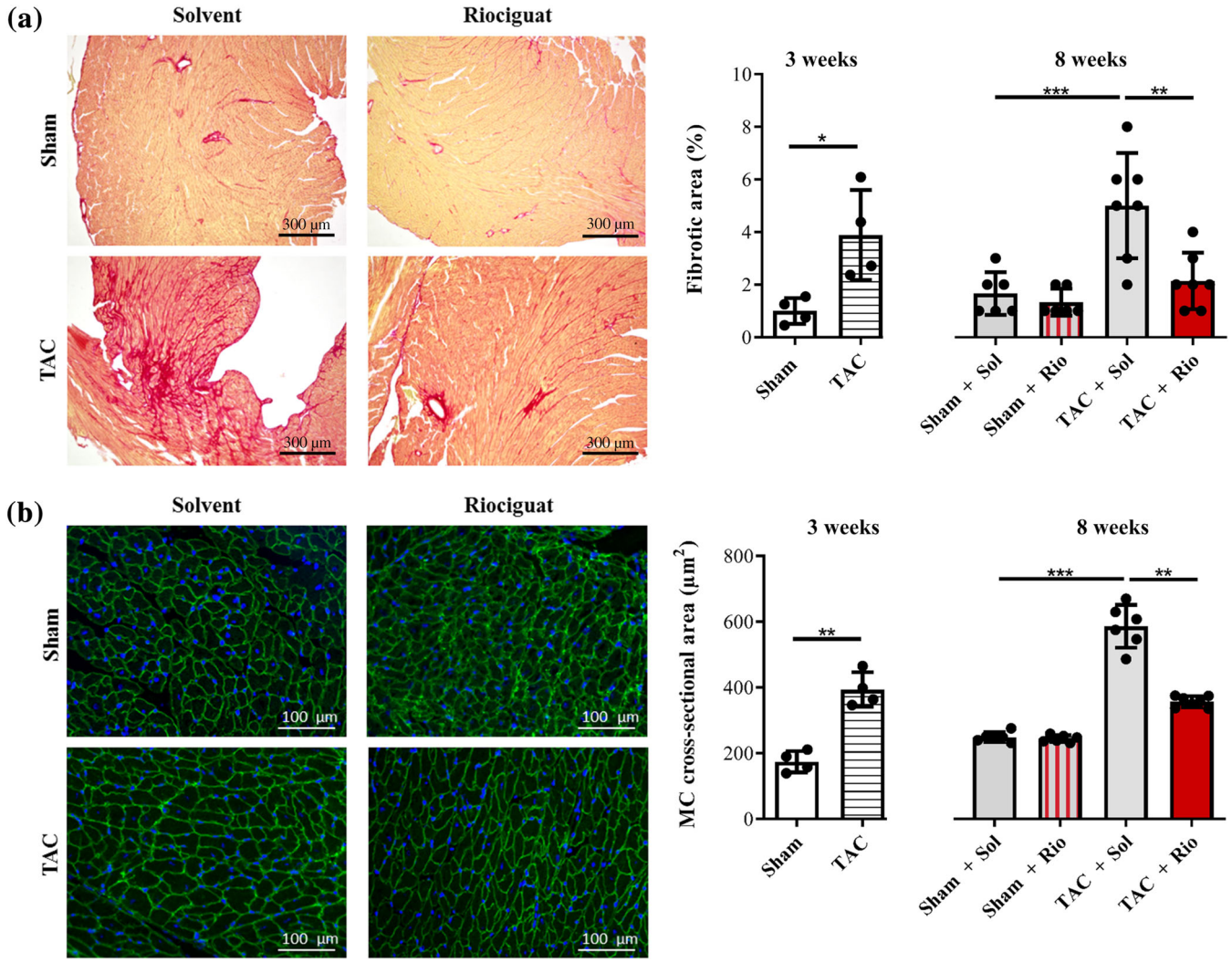

FIGURE 2 Riociguat reverses transverse aortic constriction (TAC)-induced myocyte hypertrophy and interstitial fibrosis. (a) Picrosirius red staining of histological cross sections from hearts depicting interstitial fibrosis (red). Graph shows percentage of fibrotic area in hearts 3 weeks after surgery (n = 4) and 8 weeks after surgery and drug treatment (n = 6 per group). Scale bar = 300 µm. (b) Dystrophin staining (green) of histological cross sections from hearts depicting cardiomyocyte hypertrophy. Graph shows myocyte cross-sectional area 3 weeks after surgery (n = 4) and 8 weeks after surgery and drug treatment (n = 6 per group). Scale bar = 100 µm. All data are shown as mean ± SD, *P < 0.05,

expected, picrosirius red staining showed a pronounced interstitial fibrosis in the hearts of the TAC + Sol group, which was significantly reduced in the TAC + Rio group (Figure 2a). In order to show that pathological myocardial remodelling already occurred 3 weeks after TAC and before commencement of the riociguat treatment (week 3), we performed histological analyses on cross sections from hearts of mice investigated in a previous study, in which we investigated time-dependent effects of TAC on the myocardium (Rüdebusch et al., 2017). We found a significant increase in interstitial fibrosis after 3 weeks of TAC. Five weeks of riociguat treatment of TAC mice showed decreased fibrosis. Cardiomyocyte hypertrophy followed the same route: 3 weeks of TAC caused an increase in myocyte cross-sectional area, which further increased after 8 weeks of TAC. Riociguat treatment prevented myocyte hypertrophy in response to TAC (Figure 2b).

3.2 | Riociguat attenuates transverse aortic constriction (TAC)-dependent changes in LV gene expression

To understand the molecular basis of the beneficial effects of riociguat, we performed next-generation sequencing on RNA isolated out of the LV free wall of all experimental groups (n = 6 per condition) and quantified changes in myocardial gene expression. The highest number of DEGs was found in the LV of TAC + Sol compared to Sham + Sol mice. Specifically, the expression of 3,427 genes was significantly changed due to LV pressure overload (Figure 3a), of which 1,871 genes were up-regulated and 1,556 genes were down-regulated (Figure S3). In contrast, only 2,487 genes (1,001 up-regulated and 1,486 down-regulated) were differentially regulated in riociguat-treated TAC mice (Figure 3a). The

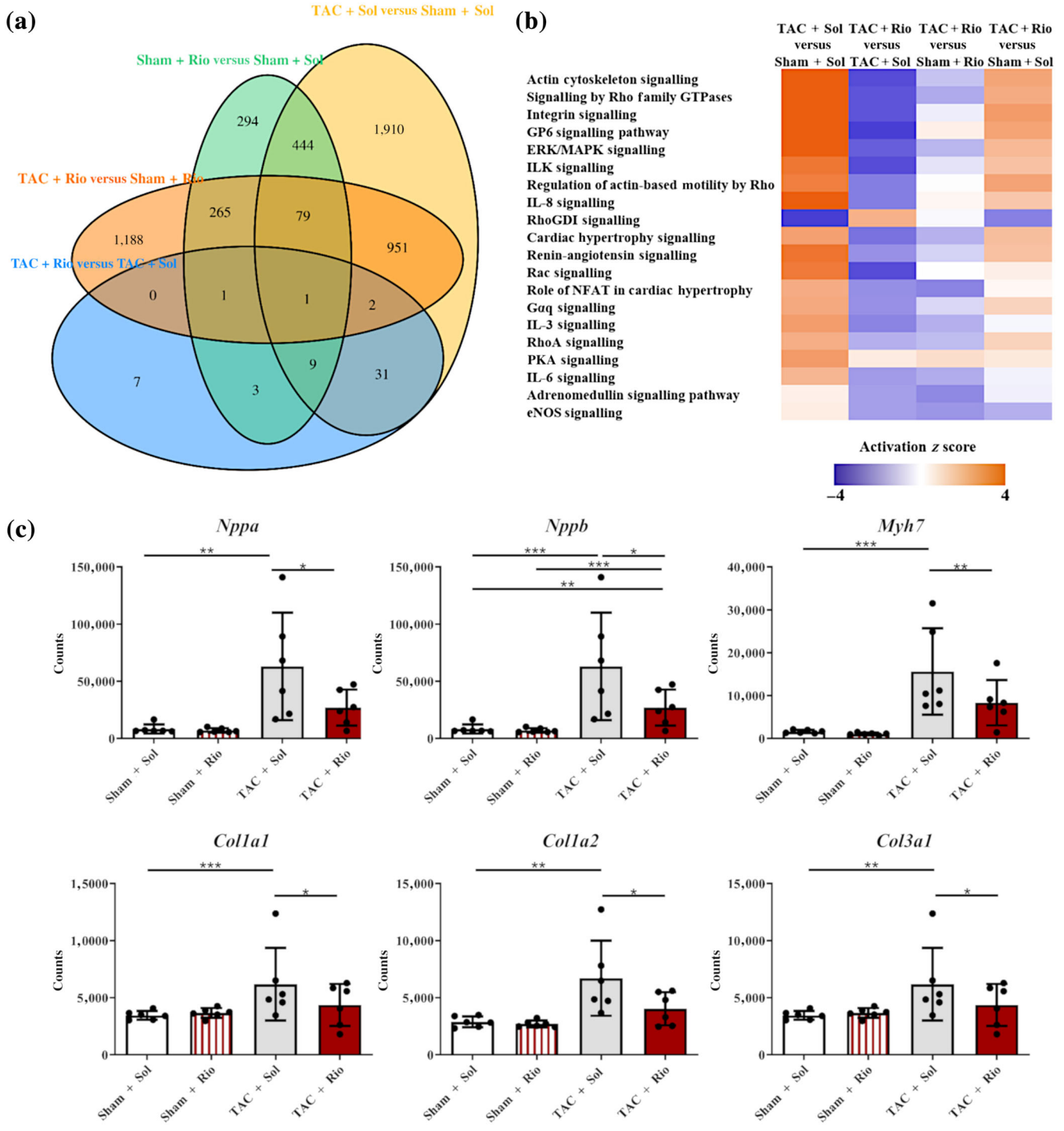

FIGURE 3 Riociguat reverses transverse aortic constriction (TAC)-induced expression of cardiac stress markers. (a) Venn diagram showing the number of 1.2-fold up-regulated and down-regulated genes and their overlap in hearts of TAC- and sham-operated and solvent- and riociguat-treated mice. The numbers of differentially expressed genes for each condition are shown. (b) Ingenuity® Pathway Analysis (IPA®) based canonical pathway analysis of differentially expressed genes in each condition. A positive *z* score predicts activation (orange); a negative score (purple) predicts inhibition of the pathway. (c) Gene expression of natriuretic peptide A (*Nppa*), natriuretic peptide B (*Nppb*), myosin heavy chain 7 (*Myh7*) and collagens 1 and 3 (*Col1a1*, *Col1a2* and *Col3a1*). Riociguat inhibited the expression of heart failure associated and remodelling genes induced by TAC. $n = 6$ per group. Data are shown as mean ± SD. $^*P < 0.05$

comparison of TAC + Rio versus TAC + Sol showed 54 DEGs (13 up-regulated and 41 down-regulated) (Figures 3a and S3). To uncover the biological pathways involved in the favourable effects of riociguat, we conducted an Ingenuity® Pathway Analysis (IPA) of the DEGs regarding their enrichment and impact on the activation or inhibition of biological pathways (Figure 3b). Pressure overload

(TAC + Sol vs. Sham + Sol) was associated with the activation of pathways (positive IPA®-derived activity *z* score), which are associated with tissue and cell structure such as actin cytoskeleton signalling and integrin signalling, and cardiac stress response such as cardiac hypertrophy signalling and renin-angiotensin signalling. Riociguat treatment inhibited these pathways, resulting in a negative *z* score (TAC + Rio vs. TAC + Sol). Interestingly, the TAC-induced activation of further pathways was attenuated as well and showed a lower *z* score when riociguat was administered (TAC + Rio vs. Sham + Sol). In particular, expression of genes associated with hypertrophy and heart failure such as **natriuretic peptide A** (*Nppa*), **natriuretic peptide B** (*Nppb*), myosin heavy chain 7 (*Myh7*) and collagens 1 and 3 (***Colla1***, *Col1a2* and *Col3a1*) was increased in the TAC + Sol group when compared to sham (Sham + Sol or Sham + Rio). This up-regulation was significantly inhibited when TAC animals were treated with riociguat (Figure 3c). Since we focused on the treatment effects of riociguat at the experimental endpoint, we have not performed analyses at the 21-day time point when heart failure was detectable and riociguat treatment was started. However, in a former study (Rüdebusch et al., 2017), we sequentially analysed the gene expression after TAC by microarray (Supporting Information Methods). Comparing analyses showed that many changes in gene expression we saw after 56 days of TAC (TAC solvent group) were also detectable after 21 days of TAC (our earlier study). This includes the activation or inhibition of critical pathways as well as the gene expression of heart failure marker genes (Figures S4 and S5). Although these data were not obtained in the same experiment and used different methods of gene expression analyses, they support our observation that riociguat has beneficial effects on the heart failure-associated gene expression signature.

To reveal the effect of sGC stimulation on gene expression pattern in diseased hearts, we searched for genes in the individual TAC samples and found 100 genes that were influenced by riociguat (Figure 4a). Specifically, we observed an enrichment of genes associated with oxidative phosphorylation, such as

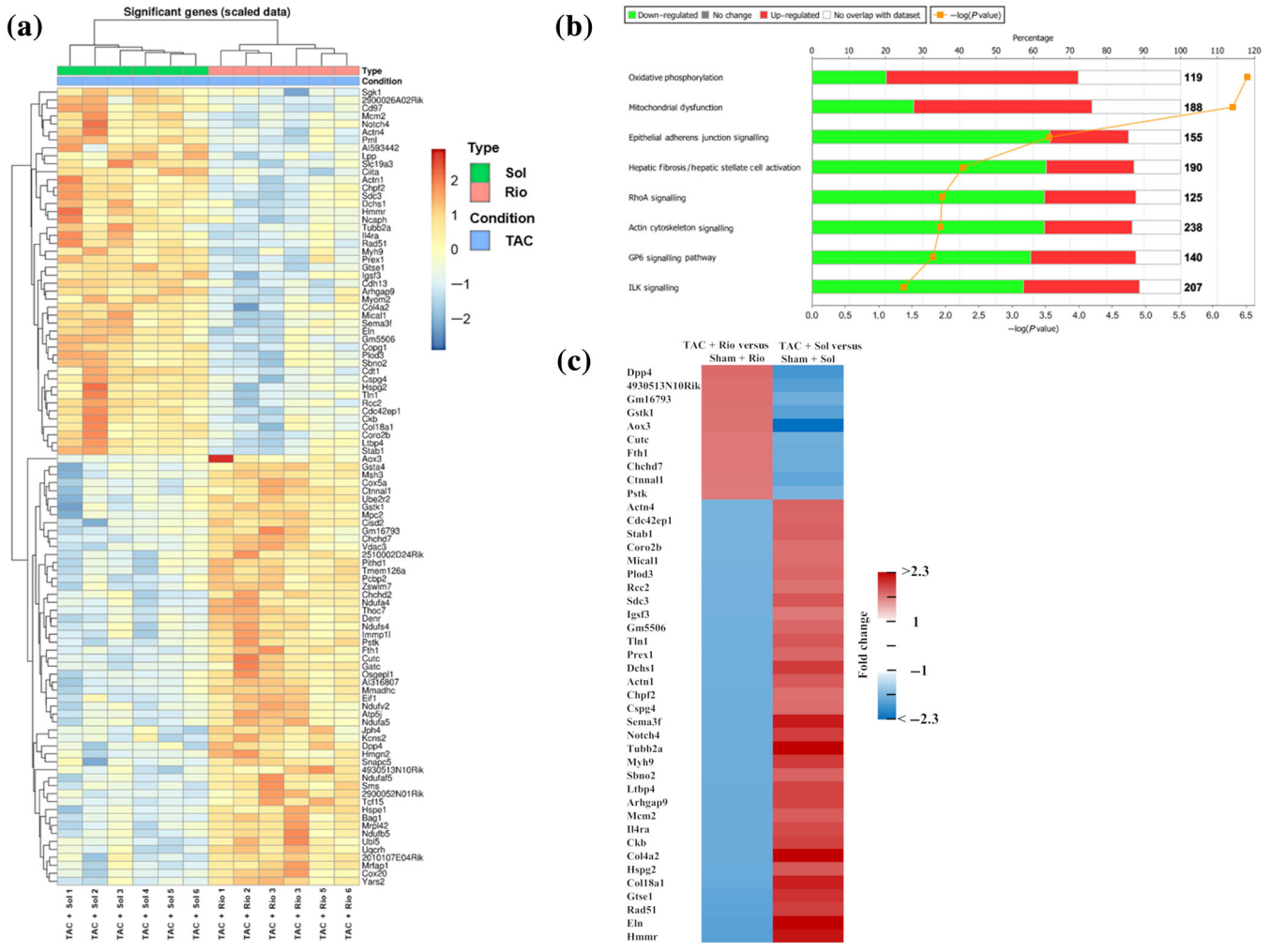

FIGURE 4 Differentially expressed genes. (a) The heat map shows scaled expression values of the differentially expressed genes for transverse aortic constriction (TAC) + Rio versus TAC + Sol in the individual samples. (b) Enrichment analysis (Ingenuity® Pathway Analysis) of differentially expressed genes for TAC + Rio versus TAC + Sol. (c) Heat map of genes regulated in both TAC + Rio versus TAC + Sol and TAC + Sol versus Sham + Sol condition

cytochrome c oxidase subunit 5A (*Cox5a*), voltage-dependent anion channel 3 (*Vdac3*) and various subunits of NADH–ubiquinone oxidoreductase (*Ndufa5*, *Ndufa 4* and *Ndufa V2*) (Figure 4b). Of particular interest was the question whether riociguat had an impact on the expression of those genes that exhibited a differential expression of at least 20% after TAC. We therefore compared TAC + Sol versus Sham + Sol and TAC + Rio versus TAC + Sol and found 43 genes (Figure 4b), regulated in both conditions. In this subset, all genes showed a reverse regulation in the TAC + Rio group, notably genes associated with actin cytoskeleton signalling such as actinin α 1 and 4 (*Actn1* and *Actn4*), myosin heavy chain 9 (*Myh 9*) and talin1 (*Tln1*), which were down-regulated in response to sGC stimulation (Figure 4c).

3.3 | Riociguat reduces fibroblast proliferation and myocyte hypertrophy in vitro

To determine whether riociguat counteracts the effects of hypertrophic agents on a cellular level, we tested its effects on fibroblasts and myocytes in culture. Since IPA® analysis revealed an activation of the renin-angiotensin signalling by TAC, which was inhibited by riociguat, we used Ang II for these experiments. Proliferation of neonatal rat cardiac fibroblasts was increased after treatment with Ang II (10 nM, 48 h) (Figure 5a). On the other hand, riociguat (100 nM) treatment ameliorated the Ang II-induced fibroblast proliferation, which was in accordance with its anti-fibrotic effects seen *in vivo*. In addition, we examined whether

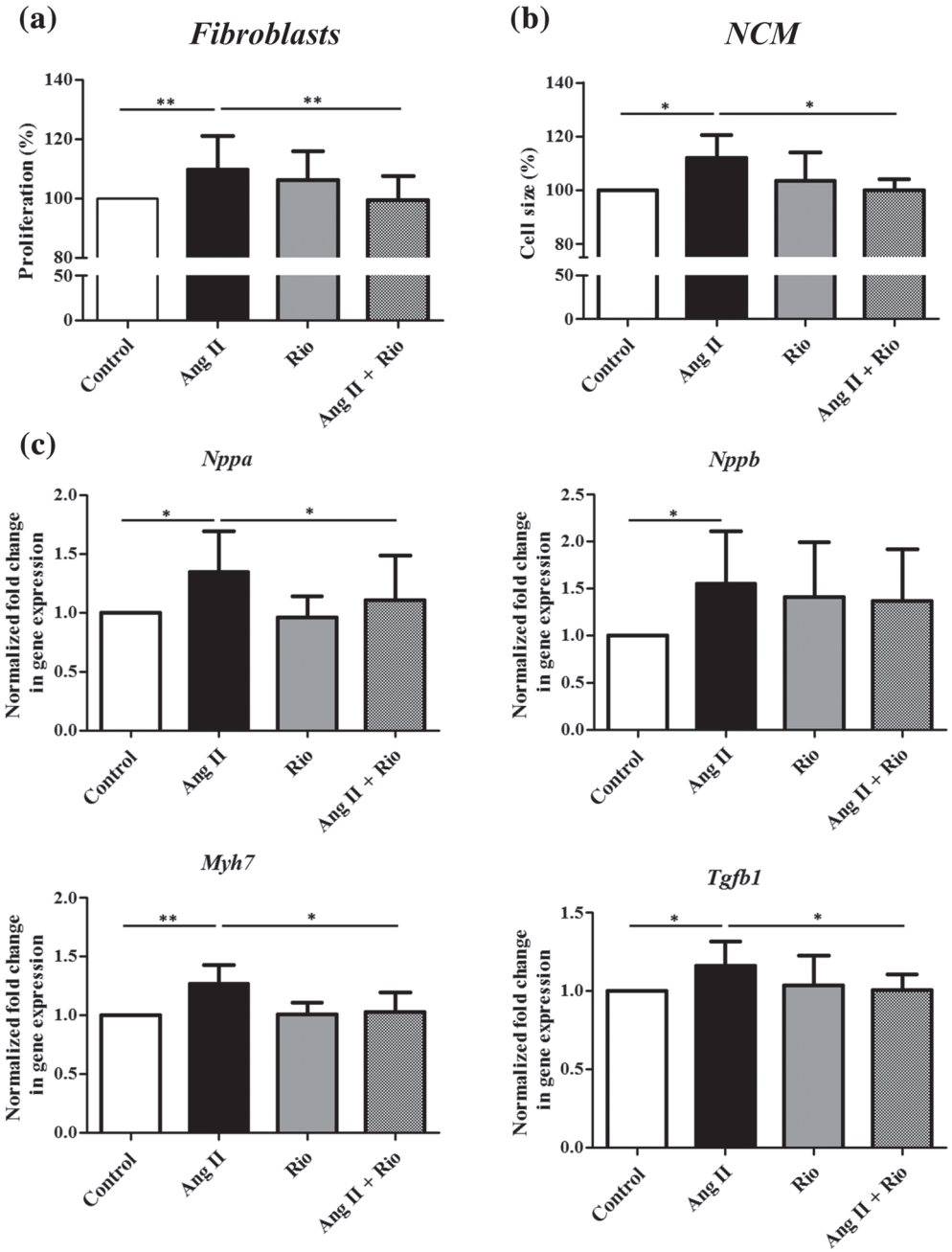

FIGURE 5 Riociguat prevents angiotensin II-induced proliferation of fibroblasts and cardiomyocyte hypertrophy in vitro. (a) Riociguat (Rio) attenuated angiotensin II (Ang II)-induced proliferation of rat ventricular fibroblasts. *n* = 8. (b) Riociguat reduced Ang II-induced hypertrophy in neonatal rat cardiomyocytes (NCMs). *n* = 6. (c) Riociguat inhibited Ang II-induced expression of natriuretic peptide A (*Nppa*), natriuretic peptide B (*Nppb*), myosin heavy chain 7 (*Myh7*) and TGF1 (*Tgfb1*) in NCMs. Gene expression analysis was performed by NanoString Technologies®. *n* = 6. All data are shown as mean ± SD. *$P < 0.05$

riociguat inhibits Ang II-induced cardiomyocyte hypertrophy *in vitro*. As expected, Ang II (10 nM) treatment of NCM caused an increase in cell size indicative for myocyte hypertrophy (Figure 5b). Ang II-induced NCM hypertrophy was accompanied by a significant increase of *Nppa*, *Nppb*, *Myh7* and *Tgfb1* expression (Figure 5c). Riociguat (100 nM) inhibited Ang II-induced NCM hypertrophy (Figure 5b) and Ang II-induced expression of *Nppa*, *Myh7* and *Tgfb1*, but not of *Nppb* (Figure 5c).

In addition, HL-1-cells (immortalized mouse atrial cardiomyocytes, RRID:CVCL_0303) were tested to validate the anti-hypertrophic effects. Here, like in NCM, riociguat attenuated the hypertrophic response to Ang II stimulation (Figure S6).

4 | DISCUSSION

The NO–sGC–cGMP pathway presents a key regulator for cardiovascular function and its impairment leads to vascular dysfunction and pathological changes in the heart such as fibrosis and hypertrophy (Sandner, 2018). This cascade is therefore of particular interest in the treatment of heart failure (Gheorghiade et al., 2013). First randomized controlled trials investigated the effects of sGC stimulators in patients with heart failure with reduced ejection fraction (HRrEF) (Armstrong et al., 2018; Bonderman et al., 2013; Gheorghiade et al., 2015; Pieske et al., 2014). The Left Ventricular Systolic Dysfunction Associated with Pulmonary Hypertension Riociguat Trial study showed that riociguat improves cardiac index and quality of life in patients with heart failure with reduced ejection fraction and secondary pulmonary hypertension (Bonderman et al., 2013). Riociguat has a moderate half-life in different species and this pharmacokinetic profile translated into a three times daily dosing regimen in patients (Frey et al., 2018; Sandner et al., 2018). As a result of an optimization approach to identify orally bioavailable sGC stimulators with a longer duration of action than riociguat, **vericiguat**, a novel sGC stimulator with optimized pharmacokinetic properties allowing once-daily dosing, was developed (Sandner et al., 2018). The phase IIb study Soluble Guanylate Cyclase Stimulator in Heart Failure with Reduced Ejection Fraction Study (SOCRATES-REDUCED) investigated the effects of different doses of the sGC stimulator vericiguat on N-terminal pro-B-type natriuretic peptide (NT-proBNP) in patients with heart failure with reduced ejection fraction (Gheorghiade et al., 2015). Whereas in a pooled analysis of the three highest doses of vericiguat, no significant change in NT-proBNP levels was observed after 12 weeks of treatment, a secondary analysis revealed a significant reduction of NT-proBNP levels by the highest vericiguat dose (Gheorghiade et al., 2015). In addition, exploratory analyses showed a numerical reduction in cardiovascular death and heart failure hospitalization (Gheorghiade et al., 2015). Based on these encouraging findings, the phase III Vericiguat Global Study in Subjects with Heart Failure with Reduced Ejection Fraction (VICTORIA) trial investigated the effects of vericiguat on the primary outcome death from cardiovascular causes or first hospitalization for heart failure hospitalization in heart failure with reduced ejection fraction patients (Armstrong et al., 2018). In this trial, the incidence of the primary outcome was significantly reduced at a median of 10.8 months among those patients who received vericiguat compared to those who received placebo (Armstrong et al., 2020).

In our experimental study, we focused on the influence of sGC stimulation on experimental heart failure and subsequently on the changes in myocardial gene expression. We used the TAC model, which ensured a permanent mechanical haemodynamic stress stimulus to the heart eventually causing heart failure. Regarding the riociguat treatment, we have chosen an experimental strategy that parallels the clinical situation. Accordingly, we started the riociguat treatment at a time point when LV function was already reduced and pathological hypertrophy and interstitial fibrosis were established (Rüdebusch et al., 2017). We found that riociguat prevented worsening of systolic LV function and reduced LV remodelling. During riociguat treatment, the LVEF recovered and the ventricular enlargement in systole improved. A significant change of the diastolic volume could not be detected, which may be due to the short observation period. LV pressure overload is associated with increased collagen deposition, which leads to fibrosis and subsequently to increased wall stiffness and impairment of cardiac function (Segura, Frazier, & Buja, 2014). Riociguat decreased TAC-induced interstitial fibrosis and reduced collagen gene expression in heart tissue *in vivo* and attenuated fibroblast proliferation *in vitro*. These anti-fibrotic effects are in line with findings on sGC stimulation in various models of hypertrophy and heart failure (Fraccarollo et al., 2014; Geschka et al., 2011; Masuyama et al., 2009; Pradhan et al., 2016; Sharkovska et al., 2010). Thus, in rat models of hypertension and of chronic cardiac volume overload, riociguat increased systolic heart function and survival and reduced hypertension and cardiac fibrosis (Geschka et al., 2011; Sharkovska et al., 2010). Furthermore, riociguat has been shown to attenuate LV remodelling after myocardial infarction in mice (Methner et al., 2013), to improve donor organ function in rat heart transplantation (Benke et al., 2020) and showed positive effects on LVFS and interstitial fibrosis after TAC (Pradhan et al., 2016). In addition to the former studies (Pradhan et al., 2016), we showed that riociguat improved LVFS, LVEF and LVESV and not only reduced fibrosis but also LV hypertrophy in response to TAC in vivo. Furthermore, it reduced cardiomyocyte hypertrophy in response to Ang II *in vitro*. Similar effects on cardiomyocytes were reported with other sGC activators and were evident in the absence of confounding haemodynamic factors (Irvine et al., 2012; Sandner, 2018). In our study, we found that the beneficial effects of sGC stimulation were associated with favourable changes in gene expression. In general, fewer genes were differentially regulated in TAC hearts when the mice were treated with riociguat, which indicates that riociguat treatment resulted in reduced cardiac stress response. This hypothesis is further supported by our observation that riociguat attenuated activation of the fetal gene program (Barry et al., 2008; Fraccarollo et al., 2014) in the LV of TAC-operated mice and in Ang II-treated NCM. Furthermore, we identified 43 genes that were differentially regulated by pressure overload whose expression patterns were reversed by riociguat. In

particular, genes involved in cytoskeleton signalling and cell structure showed a reverted regulation, suggesting a beneficial role of sGC stimulation in restauration of LV function. Activation of additional stress-activated pathways was reduced by sGC stimulation, suggesting that riociguat inhibits heart failure-associated gene expression and prevents pathological remodelling.

Targeting cGMP for treatment of heart failure is a major topic of clinical research (Emdin et al., 2020). Experimental studies indicate that cGMP and cGMP-dependent PK type I (cGKI/PKG) may ameliorate cardiac hypertrophy, fibrosis and heart failure (Hofmann, 2018). Several studies showed cardioprotective effects of the modulation of the NO–sGC–cGMP pathway, either by pharmacological modulators of NO–GC (Kolijn et al., 2020; Methner, Buonincontri, et al., 2013; Pradhan et al., 2016; Salloum et al., 2012) or inhibitors of cGMP degrading PDEs (Blanton et al., 2012; Gong et al., 2014; Hofmann, 2018; Methner et al., 2013; Nagayama et al., 2009). If these effects arise from PKG activation or if other downstream effectors are involved warrants further investigation (Bork, Molina, & Nikolaev, 2019; Frankenreiter et al., 2017; Menges et al., 2019). In this context, the role of cGKI in myocardial hypertrophy is under debate. Interestingly, deletion of cGKIα in experimental animals did not affect cardiac hypertrophy induced by **isoprenaline** or TAC (Lukowski et al., 2010).

4.1 | Limitation

In order to detect cardiovascular side effects of riociguat, we measured heart rate (Figure 1c) and aortic peak pressure, which was calculated from pulse wave Doppler recorded peak aortic velocity (Harris & Kuppurao, 2016). However, invasive haemodynamic monitoring was not available to measure changes in BP in the animals. Nevertheless, despite constant pressure overload by TAC and, consequently, constantly increased LV afterload, one may argue that peripheral vascular effects may have contributed in part to the beneficial effects of sGC stimulation in our heart failure model. Interestingly, however, our *in vitro* experiments with NCMs and fibroblasts indicate that sGC stimulation directly counteracts myocyte hypertrophy and fibroblast proliferation, independently of any haemodynamic changes.

In our experimental approach, we analysed the gene expression of the whole LV, which includes various cell types. The differential effects on a specific cell type were not investigated *in vivo*. Furthermore, it is not possible to conclude which specific gene regulation in response to sGC stimulation is causative for protection in heart failure. Relating thereto, a complex interplay in the network of gene regulation takes place and will need extension of *in vitro* and *in vivo* analyses.

5 | CONCLUSION

Our work shows that sGC stimulation with riociguat has beneficial effects on pathological cardiac remodelling. Riociguat treatment improved cardiac function, reversed hypertrophy, decreased fibrosis and attenuated alterations of gene expression patterns in the LV of mice during heart failure induced by chronic pressure overload.

AUTHOR CONTRIBUTIONS

J.R. designed the research study, conducted experiments, acquired data, analysed data and wrote the manuscript; A.B., L.F. and K.G. conducted experiments; N.N. and L.K. performed bioinformatics analyses; K.K. performed histological analyses; G.E. and T.M. performed RNA sequencing; J.F. designed the research study and wrote the manuscript; S.B.F. supervised and designed the research study and wrote the manuscript.

CONFLICT OF INTEREST

Dr. Felix has received consulting fees and speaker honorarium by Bayer Health Care (minor). All other authors have declared that no conflict of interest exists.

DECLARATION OF TRANSPARENCY AND SCIENTIFIC RIGOUR

This Declaration acknowledges that this paper adheres to the principles for transparent reporting and scientific rigour of preclinical research as stated in the *BJP* guidelines for Design & Analysis, Immunoblotting and Immunochemistry and Animal Experimentation, and as recommended by funding agencies, publishers and other organizations engaged with supporting research.

DATA AVAILABILITY STATEMENT

The data that support the findings of this study are available from the corresponding author upon reasonable request.

REFERENCES

Alexander, S. P. H., Christopoulos, A., Davenport, A. P., Kelly, E., Mathie, A., Peters, J. A., … Pawson, A. J. (2019). The Concise Guide to PHARMACOLOGY 2019/20: G protein-coupled receptors. *British Journal of Pharmacology*, *176*(Suppl 1), S21–S141. https://doi.org/10.1111/bph.14748

Ambrosy, A. P., Fonarow, G. C., Butler, J., Chioncel, O., Greene, S. J., Vaduganathan, M., … Gheorghiade, M. (2014). The global health and economic burden of hospitalizations for heart failure: Lessons learned from hospitalized heart failure registries. *Journal of the American College of Cardiology*, *63*(12), 1123–1133. https://doi.org/10.1016/j.jacc.2013.11.053

Armstrong, P. W., Pieske, B., Anstrom, K. J., Ezekowitz, J., Hernandez, A. F., Butler, J., … Group, V. S. (2020). Vericiguat in patients with heart failure and reduced ejection fraction. *The New England Journal of Medicine*, *382*, 1883–1893. https://doi.org/10.1056/NEJMoa1915928

Armstrong, P. W., Roessig, L., Patel, M. J., Anstrom, K. J., Butler, J., Voors, A. A., … O'Connor, C. M. (2018). A multicenter, randomized, double-blind, placebo-controlled trial of the efficacy and safety of the oral soluble guanylate cyclase stimulator: The VICTORIA trial. *JACC Heart Fail*, *6*(2), 96–104. https://doi.org/10.1016/j.jchf.2017.08.013

Barry, S. P., Davidson, S. M., & Townsend, P. A. (2008). Molecular regulation of cardiac hypertrophy. *The International Journal of Biochemistry & Cell Biology*, *40*(10), 2023–2039. https://doi.org/10.1016/j.biocel.2008.02.020

Benke, K., Nemeth, B. T., Sayour, A. A., Stark, K. A., Olah, A., Ruppert, M., … Radovits, T. (2020). Stimulation of soluble guanylate cyclase improves donor organ function in rat heart transplantation. *Scientific Reports*, *10*(1), 5358. https://doi.org/10.1038/s41598-020-62156-y

Blanton, R. M., Takimoto, E., Lane, A. M., Aronovitz, M., Piotrowski, R., Karas, R. H., … Mendelsohn, M. E. (2012). Protein kinase G Iα inhibits pressure overload-induced cardiac remodeling and is required for the cardioprotective effect of sildenafil in vivo. *Journal of the American Heart Association*, *1*(5), e003731. https://doi.org/10.1161/JAHA.112.003731

Bonderman, D., Ghio, S., Felix, S. B., Ghofrani, H. A., Michelakis, E., Mitrovic, V., … Left Ventricular Systolic Dysfunction Associated With Pulmonary Hypertension Riociguat Trial Study, G. (2013). Riociguat for patients with pulmonary hypertension caused by systolic left ventricular dysfunction: A phase IIb double-blind, randomized, placebo-controlled, dose-ranging hemodynamic study. *Circulation*, *128*(5), 502–511. https://doi.org/10.1161/CIRCULATIONAHA.113.001458

Bork, N. I., Molina, C. E., & Nikolaev, V. O. (2019). cGMP signalling in cardiomyocyte microdomains. *Biochemical Society Transactions*, *47*(5), 1327–1339. https://doi.org/10.1042/BST20190225

Chen, Z., Liu, J., Ng, H. K., Nadarajah, S., Kaufman, H. L., Yang, J. Y., & Deng, Y. (2011). Statistical methods on detecting differentially expressed genes for RNA-seq data. *BMC Systems Biology*, *5*, S1. https://doi.org/10.1186/1752-0509-5-S3-S1

Curtis, M. J., Alexander, S., Cirino, G., Docherty, J. R., George, C. H., Giembycz, M. A., … Ahluwalia, A. (2018). Experimental design and analysis and their reporting II: Updated and simplified guidance for authors and peer reviewers. *British Journal of Pharmacology*, *175*(7), 987–993. https://doi.org/10.1111/bph.14153

Dees, C., Beyer, C., Distler, A., Soare, A., Zhang, Y., Palumbo-Zerr, K., … Distler, J. H. (2015). Stimulators of soluble guanylate cyclase (sGC) inhibit experimental skin fibrosis of different aetiologies. *Annals of the Rheumatic Diseases*, *74*(8), 1621–1625. https://doi.org/10.1136/annrheumdis-2014-206809

Emdin, M., Aimo, A., Castiglione, V., Vergaro, G., Georgiopoulos, G., Saccaro, L. F., … Senni, M. (2020). Targeting cyclic guanosine monophosphate to treat heart failure: JACC review topic of the week. *Journal of the American College of Cardiology*, *76*(15), 1795–1807. https://doi.org/10.1016/j.jacc.2020.08.031

Fielitz, J., Hein, S., Mitrovic, V., Pregla, R., Zurbrugg, H. R., Warnecke, C., … Regitz-Zagrosek, V. (2001). Activation of the cardiac renin-angiotensin system and increased myocardial collagen expression in human aortic valve disease. *Journal of the American College of Cardiology*, *37*(5), 1443–1449. https://doi.org/10.1016/s0735-1097(01)01170-6

Fielitz, J., Kim, M. S., Shelton, J. M., Qi, X., Hill, J. A., Richardson, J. A., … Olson, E. N. (2008). Requirement of protein kinase D1 for pathological cardiac remodeling. *Proceedings of the National Academy of Sciences of the United States of America*, *105*(8), 3059–3063. https://doi.org/10.1073/pnas.0712265105

Fraccarollo, D., Galuppo, P., Motschenbacher, S., Ruetten, H., Schafer, A., & Bauersachs, J. (2014). Soluble guanylyl cyclase activation improves progressive cardiac remodeling and failure after myocardial infarction. Cardioprotection over ACE inhibition. *Basic Research in Cardiology*, *109*(4), 421. https://doi.org/10.1007/s00395-014-0421-1

Frankenreiter, S., Bednarczyk, P., Kniess, A., Bork, N. I., Straubinger, J., Koprowski, P., … Lukowski, R. (2017). cGMP-elevating compounds and ischemic conditioning provide cardioprotection against ischemia and reperfusion injury via cardiomyocyte-specific BK channels. *Circulation*, *136*(24), 2337–2355. https://doi.org/10.1161/CIRCULATIONAHA.117.028723

Frey, R., Becker, C., Saleh, S., Unger, S., van der Mey, D., & Muck, W. (2018). Clinical pharmacokinetic and pharmacodynamic profile of riociguat. *Clinical Pharmacokinetics*, *57*(6), 647–661. https://doi.org/10.1007/s40262-017-0604-7

George, C. H., Stanford, S. C., Alexander, S., Cirino, G., Docherty, J. R., Giembycz, M. A., … Ahluwalia, A. (2017). Updating the guidelines for data transparency in the *British Journal of Pharmacology*—Data sharing and the use of scatter plots instead of bar charts. *British Journal of Pharmacology*, *174*(17), 2801–2804. https://doi.org/10.1111/bph.13925

Geschka, S., Kretschmer, A., Sharkovska, Y., Evgenov, O. V., Lawrenz, B., Hucke, A., … Stasch, J. P. (2011). Soluble guanylate cyclase stimulation prevents fibrotic tissue remodeling and improves survival in salt-sensitive Dahl rats. *PLoS ONE*, *6*(7), e21853. https://doi.org/10.1371/journal.pone.0021853

Gheorghiade, M., Greene, S. J., Butler, J., Filippatos, G., Lam, C. S., Maggioni, A. P., … Coordinators (2015). Effect of vericiguat, a soluble guanylate cyclase stimulator, on natriuretic peptide levels in patients with worsening chronic heart failure and reduced ejection fraction: The SOCRATES-REDUCED randomized trial. *JAMA*, *314*(21), 2251–2262. https://doi.org/10.1001/jama.2015.15734

Gheorghiade, M., Marti, C. N., Sabbah, H. N., Roessig, L., Greene, S. J., Bohm, M., … Academic Research Team in Heart, F. (2013). Soluble guanylate cyclase: A potential therapeutic target for heart failure. *Heart Failure Reviews*, *18*(2), 123–134. https://doi.org/10.1007/s10741-012-9323-1

Ghofrani, H. A., Humbert, M., Langleben, D., Schermuly, R., Stasch, J. P., Wilkins, M. R., & Klinger, J. R. (2017). Riociguat: Mode of action and clinical development in pulmonary hypertension. *Chest*, *151*(2), 468–480. https://doi.org/10.1016/j.chest.2016.05.024

Gong, W., Yan, M., Chen, J., Chaugai, S., Chen, C., & Wang, D. (2014). Chronic inhibition of cyclic guanosine monophosphate-specific phosphodiesterase 5 prevented cardiac fibrosis through inhibition of transforming growth factor β-induced Smad signaling. *Frontiers in Medicine*, *8*(4), 445–455. https://doi.org/10.1007/s11684-014-0378-3

Harris, P., & Kuppurao, L. (2016). Quantitative Doppler echocardiography. *Bja Education*, *16*(2), 46–52. https://doi.org/10.1093/bjaceaccp/mkv015

Hofmann, F. (2018). A concise discussion of the regulatory role of cGMP kinase I in cardiac physiology and pathology. *Basic Research in Cardiology*, *113*(4). https://doi.org/10.1007/s00395-018-0690-1

Irvine, J. C., Ganthavee, V., Love, J. E., Alexander, A. E., Horowitz, J. D., Stasch, J. P., … Ritchie, R. H. (2012). The soluble guanylyl cyclase activator bay 58-2667 selectively limits cardiomyocyte hypertrophy. *PLoS ONE*, *7*(11), e44481. https://doi.org/10.1371/journal.pone.0044481

Kolijn, D., Kovacs, A., Herwig, M., Lodi, M., Sieme, M., Alhaj, A., … Hamdani, N. (2020). Enhanced cardiomyocyte function in hypertensive rats with diastolic dysfunction and human heart failure patients after acute treatment with soluble guanylyl cyclase (sGC) activator. *Frontiers in Physiology*, *11*(345). https://doi.org/10.3389/fphys.2020.00345

Lilley, E., Stanford, S. C., Kendall, D. E., Alexander, S. P., Cirino, G., Docherty, J. R., … Ahluwalia, A. (2020). ARRIVE 2.0 and the *British Journal of Pharmacology*: Updated guidance for 2020. *British Journal of Pharmacology*, *177*(16), 3611–3616. https://doi.org/10.1111/bph.15178

Lukowski, R., Rybalkin, S. D., Loga, F., Leiss, V., Beavo, J. A., & Hofmann, F. (2010). Cardiac hypertrophy is not amplified by deletion of cGMP-dependent protein kinase I in cardiomyocytes. *Proceedings of the National Academy of Sciences of the United States of America*, *107*(12), 5646–5651. https://doi.org/10.1073/pnas.1001360107

Masuyama, H., Tsuruda, T., Sekita, Y., Hatakeyama, K., Imamura, T., Kato, J., … Kitamura, K. (2009). Pressure-independent effects of pharmacological stimulation of soluble guanylate cyclase on fibrosis in pressure-overloaded rat heart. *Hypertension Research*, *32*(7), 597–603. https://doi.org/10.1038/hr.2009.64

Menges, L., Krawutschke, C., Fuchtbauer, E. M., Fuchtbauer, A., Sandner, P., Koesling, D., & Russwurm, M. (2019). Mind the gap (junction): cGMP induced by nitric oxide in cardiac myocytes originates

from cardiac fibroblasts. *British Journal of Pharmacology*, *176*(24), 4696–4707. https://doi.org/10.1111/bph.14835

Methner, C., Buonincontri, G., Hu, C. H., Vujic, A., Kretschmer, A., Sawiak, S., … Krieg, T. (2013). Riociguat reduces infarct size and post-infarct heart failure in mouse hearts: Insights from MRI/PET imaging. *PLoS ONE*, *8*(12), e83910. https://doi.org/10.1371/journal.pone.0083910

Methner, C., Lukowski, R., Grube, K., Loga, F., Smith, R. A., Murphy, M. P., … Krieg, T. (2013). Protection through postconditioning or a mitochondria-targeted S-nitrosothiol is unaffected by cardiomyocyte-selective ablation of protein kinase G. *Basic Research in Cardiology*, *108*(2), 337. https://doi.org/10.1007/s00395-013-0337-1

Nagayama, T., Hsu, S., Zhang, M., Koitabashi, N., Bedja, D., Gabrielson, K. L., … Kass, D. A. (2009). Sildenafil stops progressive chamber, cellular, and molecular remodeling and improves calcium handling and function in hearts with pre-existing advanced hypertrophy caused by pressure overload. *Journal of the American College of Cardiology*, *53*(2), 207–215. https://doi.org/10.1016/j.jacc.2008.08.069

Ott, I. M., Alter, M. L., von Websky, K., Kretschmer, A., Tsuprykov, O., Sharkovska, Y., … Hocher, B. (2012). Effects of stimulation of soluble guanylate cyclase on diabetic nephropathy in diabetic eNOS knockout mice on top of angiotensin II receptor blockade. *PLoS ONE*, *7*(8), e42623. https://doi.org/10.1371/journal.pone.0042623

Percie du Sert, N., Hurst, V., Ahluwalia, A., Alam, S., Avey, M. T., Baker, M., … Würbel, H. (2020). The ARRIVE guidelines 2.0: Updated guidelines for reporting animal research. *PLoS Biology*, *18*(7), e3000410. https://doi.org/10.1371/journal.pbio.3000410

Pichl, A., Sommer, N., Bednorz, M., Seimetz, M., Hadzic, S., Kuhnert, S., … Weissmann, N. (2019). Riociguat for treatment of pulmonary hypertension in COPD: A translational study. *The European Respiratory Journal*, *53*(6), 1802445. https://doi.org/10.1183/13993003.02445-2018

Pieske, B., Butler, J., Filippatos, G., Lam, C., Maggioni, A. P., Ponikowski, P., … Coordinators (2014). Rationale and design of the SOluble guanylate Cyclase stimulatoR in heArT failurE Studies (SOCRATES). *European Journal of Heart Failure*, *16*(9), 1026–1038. https://doi.org/10.1002/ejhf.135

Ponikowski, P., Voors, A. A., Anker, S. D., Bueno, H., Cleland, J. G. F., Coats, A. J. S., … Group, E. S. C. S. D. (2016). 2016 ESC Guidelines for the diagnosis and treatment of acute and chronic heart failure: The Task Force for the diagnosis and treatment of acute and chronic heart failure of the European Society of Cardiology (ESC). Developed with the special contribution of the Heart Failure Association (HFA) of the ESC. *European Heart Journal*, *37*(27), 2129–2200. https://doi.org/10.1093/eurheartj/ehw128

Pradhan, K., Sydykov, A., Tian, X., Mamazhakypov, A., Neupane, B., Luitel, H., … Schermuly, R. T. (2016). Soluble guanylate cyclase stimulator riociguat and phosphodiesterase 5 inhibitor sildenafil ameliorate pulmonary hypertension due to left heart disease in mice. *International Journal of Cardiology*, *216*, 85–91. https://doi.org/10.1016/j.ijcard.2016.04.098

Reinke, Y., Gross, S., Eckerle, L. G., Hertrich, I., Busch, M., Busch, R., … Felix, S. B. (2015). The soluble guanylate cyclase stimulator riociguat and the soluble guanylate cyclase activator cinaciguat exert no direct effects on contractility and relaxation of cardiac myocytes from normal rats. *European Journal of Pharmacology*, *767*, 1–9. https://doi.org/10.1016/j.ejphar.2015.09.022

Reiss, C., Mindukshev, I., Bischoff, V., Subramanian, H., Kehrer, L., Friebe, A., … Walter, U. (2015). The sGC stimulator riociguat inhibits platelet function in washed platelets but not in whole blood. *British Journal of Pharmacology*, *172*(21), 5199–5210. https://doi.org/10.1111/bph.13286

Rüdebusch, J., Benkner, A., Poesch, A., Dörr, M., Völker, U., Grube, K., … Felix, S. B. (2017). Dynamic adaptation of myocardial proteome during heart failure development. *PLoS ONE*, *12*(10), e0185915. https://doi.org/10.1371/journal.pone.0185915

Rueden, C. T., Schindelin, J., Hiner, M. C., DeZonia, B. E., Walter, A. E., Arena, E. T., & Eliceiri, K. W. (2017). ImageJ2: ImageJ for the next generation of scientific image data. *BMC Bioinformatics*, *18*(1), 529. https://doi.org/10.1186/s12859-017-1934-z

Salloum, F. N., Das, A., Samidurai, A., Hoke, N. N., Chau, V. Q., Ockaili, R. A., … Kukreja, R. C. (2012). Cinaciguat, a novel activator of soluble guanylate cyclase, protects against ischemia/reperfusion injury: Role of hydrogen sulfide. *American Journal of Physiology. Heart and Circulatory Physiology*, *302*(6), H1347–H1354. https://doi.org/10.1152/ajpheart.00544.2011

Sandner, P. (2018). From molecules to patients: Exploring the therapeutic role of soluble guanylate cyclase stimulators. *Biological Chemistry*, *399*(7), 679–690. https://doi.org/10.1515/hsz-2018-0155

Sandner, P., Zimmer, D. P., Milne, G. T., Follmann, M., Hobbs, A., & Stasch, J.-P. (2018). Soluble guanylate cyclase stimulators and activators. In *Handbook of experimental pharmacology*. Berlin, Heidelberg: Springer.

Segura, A. M., Frazier, O. H., & Buja, L. M. (2014). Fibrosis and heart failure. *Heart Failure Reviews*, *19*(2), 173–185. https://doi.org/10.1007/s10741-012-9365-4

Sharkovska, Y., Kalk, P., Lawrenz, B., Godes, M., Hoffmann, L. S., Wellkisch, K., … Stasch, J. P. (2010). Nitric oxide-independent stimulation of soluble guanylate cyclase reduces organ damage in experimental low-renin and high-renin models. *Journal of Hypertension*, *28*(8), 1666–1675. https://doi.org/10.1097/HJH.0b013e32833b558c

SUPPORTING INFORMATION

Additional supporting information may be found online in the Supporting Information section at the end of this article.

How to cite this article: Rüdebusch J, Benkner A, Nath N, et al. Stimulation of soluble guanylyl cyclase (sGC) by riociguat attenuates heart failure and pathological cardiac remodelling. *Br J Pharmacol*. 2020;1–13. https://doi.org/10.1111/bph.15333